Enzyme Catalysis

Electrochemistry, AFM, and PM-IRRA Spectroscopy of Immobilized Hydrogenase: Role of a Hydrophobic Helix in Enzyme Orientation for Efficient H₂ Oxidation**

Alexandre Ciaccafava, Pascale Infossi, Marianne Ilbert, Marianne Guiral, Sophie Lecomte, Marie Thérèse Giudici-Orticoni, and Elisabeth Lojou

Nickel–iron hydrogenase ([NiFe] Hase) catalyzes hydrogen splitting into protons and electrons, and is a potential biocatalyst in fuel cells.[1] Three FeS clusters aligned as a conductive wire drive electrons from the [NiFe] active site to the surface of the enzyme, where the redox partner (including the electrode) binds. Direct enzyme connection gave access to thermodynamic and kinetic data of enzymatic reactions through direct electron transfer (DET). Mediated electron transfer (MET) allowed recreation of the physiological electron-transfer chain, and/or connection of unfavorably oriented enzymes.[2–6] Previous work demonstrated that DET or MET processes for H₂ oxidation by a soluble, O₂-sensitive [NiFe] Hase from *Desulfovibrio* species could be controlled by electrostatic interaction.[7] The presence of an acidic patch of amino acids, coupled to a dipole moment pointing towards the distal FeS cluster (positioned at the surface of the enzyme), allowed orientation of the enzyme, which turned upside down as a function of the charge on the electrochemical interface.

Recently, we reported on the electrochemistry of membrane-bound *Aquifex aeolicus* (*Aa*) [NiFe] Hase, which exhibits outstanding resistance to O₂, CO, and heat.[8–10] Efficient immobilization of this Hase was achieved on graphite electrodes, in aqueous electrolytes and ionic liquids, by encapsulation in carbon nanotube networks, or connection to a redox polymer.[11,12] In contrast to the soluble, O₂-sensitive [NiFe] Hase, no specific orientation could be obtained by electrostatic interaction for *Aa* Hase, and thus

control of the electron-transfer process was not possible. A model structure accordingly put forward a very different environment of the distal FeS cluster, with no charged amino acid patch, in accordance with the membrane anchorage.[12] We analyze herein H₂ oxidation by *Aa* Hase immobilized on self-assembled monolayers (SAMs) on gold electrodes as a function of both the length and the nature of the thiol derivative (see SI 1 and SI 2 in the Supporting Information). For the first time, AFM and polarization modulation infrared reflection adsorption (PM-IRRA) studies are reported for understanding *Aa* Hase orientation and its consequences for electron-transfer process in H₂ oxidation.

Positively charged 4-aminothiophenol (ArNH₂) and negatively charged 6-mercaptohexanoic acid (C₅COOH) SAMs both yield DET and MET processes for H₂ oxidation (Figure 1a and b), and neither process is favored over the other. A mixed process was similarly observed for H₂ oxidation at charged short-chain alkanethiols, which are known to be more disordered.[8] This strongly suggests that electroenzymatic H₂ oxidation is linked to multiple orientations of Hase on top of the charged SAMs, and not to Hase present inside possible SAM defects. The lipophilic methylene blue (MB) molecule
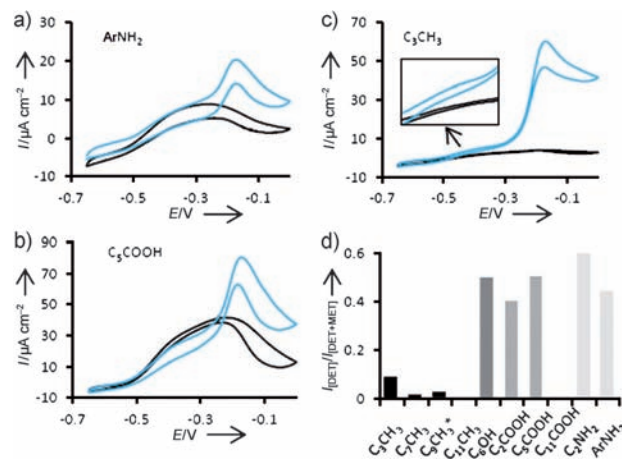
[*] A. Ciaccafava, P. Infossi, Dr. M. Ilbert, Dr. M. Guiral,
Dr. M. T. Giudici-Orticoni, Dr. E. Lojou
Bioénergétique et Ingénierie des Protéines
Institut de Microbiologie de la Méditerranée—CNRS
31 Chemin Aiguier, 13009 Marseille (France)
E-mail: lojou@ifr88.cnrs-mrs.fr

Dr. S. Lecomte
Chimie et Biologie des Membranes et Nanoobjets
CNRS-Université Bordeaux 1
2 rue Robert Escarpit, 33607 Pessac (France)

Supporting information for this article is available on the WWW under http://dx.doi.org/10.1002/anie.201107053.

Figure 1. Cyclic voltammograms (CV) for H₂ oxidation via *Aa* Hase on SAM gold electrodes before (black lines) and after (blue lines) addition of 10 μM MB. a) ArNH₂, b) C₅COOH, c) C₃CH₃, d) $I_{DET}/I_{(DET+MET)}$ ratio relative to *Aa* Hase orientation as a function of SAM properties (*: from reference [2]). The inset in c) focuses on the potential range −0.55 to −0.3 V and shows the increase in DET current after MB addition. Potentials are given versus Ag/AgCl reference electrode. 5 mVs⁻¹, 50 mM 4-(2-hydroxyethyl)-1-piperazineethanesulfonic acid (HEPES), pH 6.8, 60°C, H₂ atm.

can be incorporated into SAMs.[13] Thus, when the end-charged alkyl chain contains more than 11 methylene groups (see SI 3 in the Supporting Information), H_2 oxidation proceeds only through a MET process, in agreement with Marcus-theory long-range ET.[14]

Adsorption of *Aa* Hase on a 1-butanethiol (C_3CH_3) hydrophobic SAM mimicking the physiological environment unexpectedly results in a majority MET process (Figure 1c). This process is stable at least for one day, and the rate constant between *Aa* Hase and MB is calculated to be 78 s^{-1}. Only a weak DET process for H_2 oxidation is observed, which shows a 50% increase after addition of MB (inset of Figure 1c). The same phenomenon occurred when Toluidine Blue O was used as redox polymer matrix,[12] and is related to MB, which is incorporated in the SAM layer. Indeed, comparing the respective length of the C_3CH_3 SAM layer and MB molecule, MB can anchor *Aa* Hase at the top of the SAM in a favorable orientation for an enhanced DET process.

The $I_{DET}/I_{(DET+MET)}$ ratios obtained with *Aa* Hase adsorbed on the various SAMs (Figure 1d) highlight two distinct behaviors. On charged and neutral hydrophilic surfaces, H_2 oxidation proceeds as a mixed DET+MET process, with almost equivalent current for DET and MET processes, providing that the number of CH_2 groups in the alkyl chain is less than ten. The $I_{DET}/I_{(DET+MET)}$ ratio takes a value of around 0.5. Conversely, on hydrophobic SAMs, the MET process is largely favored, even for short alkyl chains. The $I_{DET}/I_{(DET+MET)}$ ratio is now 0.08 for C_3CH_3 SAM, a value close to that obtained in our previous work on 1-decanethiol (C_9CH_3) SAM electrodes, and far lower than that obtained at charged SAM electrodes.[8] We have thus demonstrated that favoring of MET versus DET process for H_2 oxidation at hydrophobic SAM electrodes is not related to the length, but to SAM hydrophobicity.

Immobilization of *Aa* Hase on hydrophobic C_3CH_3 SAM was examined by AFM (Figure 2). A homogeneous distribution of spheres with a mean height of 3 nm and a lateral dimension of 30 nm is observed. This gold plate exhibits an MET current characteristic for H_2 oxidation. The image features are in accordance with data collected by De Lacey et al. and are attributed to one monolayer of *Aa* Hase, the size of which is close to 5 nm.[15]

PM-IRRAS is a very sensitive method for characterizing chemical groups at the electrode surface. For the first time, it has been used to characterize Hase orientation (Figure 3). The adsorption of *Aa* Hase on the SAMs is indicated by the appearance of amide I and II bands at 1661 and 1545 cm^{-1}, respectively. The position of the former band indicates that the secondary structure of the Hase is mainly α-helix, in agreement with 40% α-helix and 15% β-sheets given by a homologous structure.[16] The shape of the amide I band of *Aa* Hase adsorbed on hydrophilic or hydrophobic surfaces, as well as on an attenuated total reflectance Ge crystal (see SI 4 in Supporting Information) is similar. Both hydrophilic and hydrophobic surfaces thus adsorb *Aa* Hase without modification of its secondary structure. However, the orientations of *Aa* Hase on the hydrophilic (Figure 3a) and hydrophobic (Figure 3b) surfaces differ. The amide I/amide II band-area ratios are clearly different, namely, 6.5 and 4 for hydrophilic
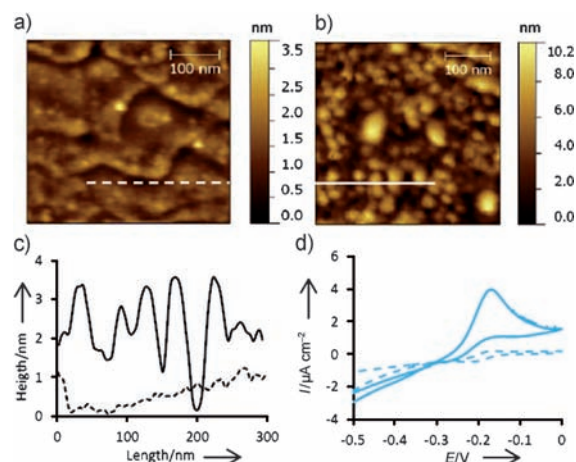

Figure 2. Noncontact-mode AFM topographic image of C_3CH_3-modified gold(111) plate a) before and b) after incubation in 1 μM *Aa* Hase. c) z-axis profiles of a) (dotted line) and b) (plain line). d) CV on C_3CH_3-modified gold(111) plate for 10 μM MB (dotted line) and for H_2 oxidation by *Aa* Hase in the presence of 10 μM MB (plain line). Potentials are given versus Ag/AgCl reference electrode. 5 mVs^{-1}, 50 mM HEPES, pH 6.8, 60°C, H_2 atmosphere.
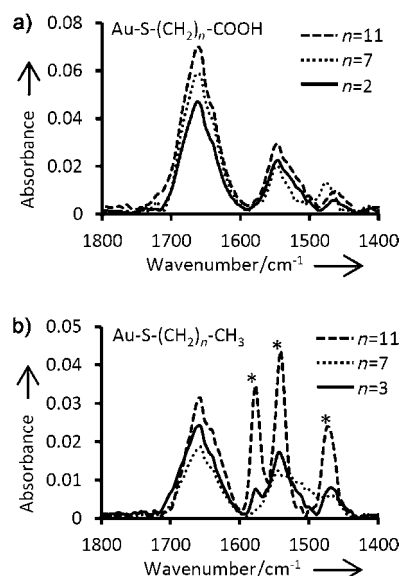

Figure 3. PM-IRRAS of *Aa* Hase on a) Au—S(CH_2)$_n$COOH and b) Au—S(CH_2)$_n$CH$_3$ surfaces. * Thin bands at 1577 and 1541 cm^{-1} are detected in addition to the amide II band (at 1542 cm^{-1}), and could be assigned to CO_3^- or HCO_3^-.

and hydrophobic surfaces, respectively. Based on previously published simulation models, we evaluated the orientation of the α-helix axis of *Aa* Hase adsorbed on SAMs by assuming that 1) all amide groups have a helical secondary structure, and 2) all helices are tilted at a similar angle to the normal of the interface.[17,18] The angle of the α-helix is around 25° for adsorption on hydrophilic surfaces and 40° for hydrophobic surfaces. We conclude that observation of an MET versus a DET+MET process for H_2 electrocatalytic oxidation according to the hydrophobicity of the surface is linked to a different orientation of *Aa* Hase. Hence, the angle obtained for

hydrophilic SAMs corresponds to a mean of multiple orientations of *Aa* Hase, while that obtained on hydrophobic SAMs is linked to a preferential orientation with the distal FeS cluster far from the electrochemical interface.

The *Aa* Hase was solubilized from the cell membrane fractions with dodecyl maltoside (DDM) neutral detergent. Although the concentration steps at the end of the purification remove the excess of detergent, it is hardly conceivable that no DDM remains surrounding the enzyme, while preserving its integrity. Thin layer chromatography (Figure 4) confirmed that diluted enzyme solution (1 μM)
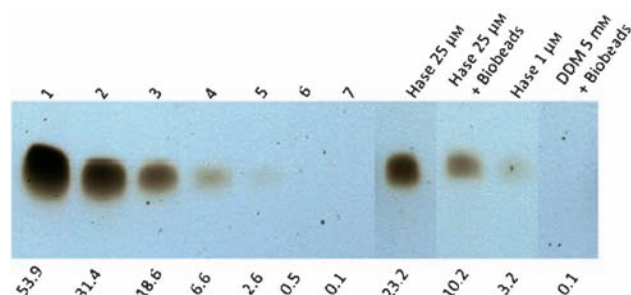

Figure 4. TLC for quantification of DDM surrounding *Aa* Hase; lanes 1 to 7: DDM calibration spots for 20, 10, 5, 2, 1, 0.2, and 0.02 mM DDM; values at the bottom correspond to the absorbance at 440 nm of each spot.

contains around 1 mM DDM. The detergent is strongly bound to the enzyme, since after treatment with Biobeads only part of the DDM is removed, in marked contrast to free DDM in solution. By mass spectrometry, a trans-membrane helix situated less than 15 Å from the distal FeS cluster is identified on solubilized *Aa* Hase.[8] It is composed of hydrophobic amino acid residues and is likely surrounded by DDM molecules, turning the domain in the vicinity of the FeS distal cluster hydrophilic. Consequently, we propose that this helix plays a key role in the orientation of hydrogenase on SAM interfaces. On hydrophobic interfaces, the FeS distal cluster remains at a distance from the electrode at which electron-transfer tunneling can not take place. On the other hand, the DDM-induced hydrophilicity of the helix, in addition to the absence of a charged patch in close proximity to the distal FeS cluster, prevents any specific orientation of the enzyme on hydrophilic electrochemical interfaces.

In summary, the efficiency toward H$_2$ oxidation of immobilized *Aa* Hase depends on the hydrophobicity of the electrochemical interface. An innovative combination of electrochemistry, AFM, and PM-IRRAS demonstrates no preferential orientation of the enzyme on hydrophilic interfaces, while hydrophobic surfaces favor one orientation with the distal FeS cluster far from the electrochemical interface. This specific orientation is driven by the presence of a trans-membrane helix surrounded by neutral detergent, and by the absence of charged residues in the close vicinity of the distal FeS cluster. Thus, on charged or hydrophilic interfaces, H$_2$ oxidation proceeds through both DET and MET processes, while on hydrophobic surfaces, H$_2$ can only be oxidized by a redox mediator (Scheme 1).
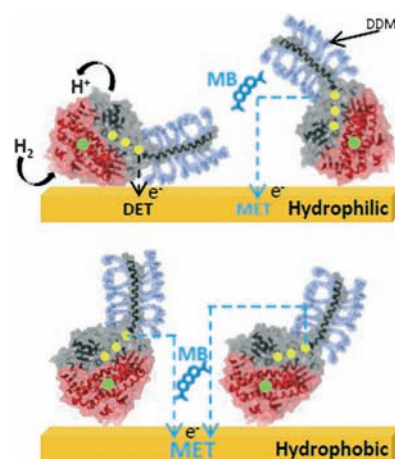
Scheme 1. The trans-membrane helix surrounded by DDM in the close vicinity of the distal FeS cluster in *Aa* Hase controls the electron-transfer process for H$_2$ oxidation. Yellow and green spheres represent FeS clusters and [NiFe] active center, respectively.

The results obtained in this work demonstrate that hydrophilic surfaces are beneficial for high performance of a future bioelectrode. High current densities at low overpotential can be reached by enzymes directly connected to the electrode, but the bioelectrode can also be run thanks to a mediated process at potentials at which Hases would be inactivated. Electrode materials are needed that allow efficient encapsulation of both the enzyme and the redox mediator, while facilitating mass transfer. Work is in progress to design such electrodes.

[1] B. Friedrich, J. Fritsch, O. Lenz, *Curr. Opin. Biotechnol.* **2011**, *22*, 358–364.

[2] E. Lojou, *Electrochim. Acta* **2011**, *56*, 10385–10397.

[3] D. Millo, P. Hildebrandt, M. Pandelia, W. Lubitz, I. Zebger, *Angew. Chem.* **2011**, *123*, 2680–2683; *Angew. Chem. Int. Ed.* **2011**, *50*, 2632–2634.

[4] M. Sezer, S. Frielingsdorf, D. Millo, N. Heidary, T. Utesch, M. A. Mroginski, B. Friedrich, P. Hildebrandt, I. Zebger, I. M. Weidinger, *J. Phys. Chem. B* **2011**, *115*, 10368–10374.

[5] S. Dementin, B. Burlat, V. Fourmond, F. Leroux, P. P. Liebgott, A. Abou Hamdan, C. Leger, M. Rousset, B. Guigliarelli, P. Bertrand, *J. Am. Chem. Soc.* **2011**, *133*, 10211–10221.

[6] E. Reisner, F. Armstrong, *Methods Mol. Biol.* **2011**, *743*, 107–117.

[7] E. Lojou, X. Luo, M. Brugna, N. Candoni, S. Dementin, M. T. Giudici-Orticoni, *J. Biol. Inorg. Chem.* **2008**, *13*, 1157–1167.

[8] X. Luo, M. Brugna, P. Infossi, M. T. Giudici-Orticoni, E. Lojou, *J. Biol. Inorg. Chem.* **2009**, *14*, 1275–1288.

[9] M. Pandelia, V. Fourmond, P. Tron-Infossi, E. Lojou, P. Bertrand, C. Leger, M. T. Giudici-Orticoni, W. Lubitz, *J. Am. Chem. Soc.* **2010**, *132*, 6991–7004.

[10] M. E. Pandelia, P. Infossi, M. T. Giudici-Orticoni, W. Lubitz, *Biochemistry* **2010**, *49*, 8873–8881.

[11] A. Ciaccafava, M. Alberola, S. Hameury, P. Infossi, M. T. Giudici-Orticoni, E. Lojou, *Electrochim. Acta* **2011**, *56*, 3359–3368.

[12] A. Ciaccafava, P. Infossi, M. T. Giudici-Orticoni, E. Lojou, *Langmuir* **2010**, *26*, 18534–18541.

[13] D. Grumelli, L. Mendez De Leo, C. Bonazzola, V. Zamlynny, E. Calvo, R. Salvarezza, *Langmuir* **2010**, *26*, 8226–8232.

[14] D. Khoshtariya, T. Dolidze, M. Shushanyan, K. Davis, D. Waldeck, R. van Eldik, *Proc. Natl. Acad. Sci. USA* **2010**, *107*, 2757–2762.

[15] C. Gutiérrez-Sánchez, D. Olea, M. Marques, V. Fernández, I. Pereira, M. Vélez, A. De Lacey, *Langmuir* **2011**, *27*, 6449–6457.

[16] E. Goormaghtigh, V. Cabiaux, J. M. Ruysschaert in *Physico-chemical Methods in the Study of Biomembranes* (Eds.: H. Hilderson, G. Ralson), Plenum, New York, **1994**, pp. 405–450.

[17] D. Blaudez, J. M. Turlet, J. Dufourcq, D. Bard, T. Buffeteau, B. Desbat, *J. Chem. Soc. Faraday Trans.* **1996**, *92*, 525–530.

[18] O. Cornut, B. Desbat, J. M. Turlet, J. Dufourcq, *Biophys. J.* **1996**, *70*, 305–312.